For example, PKA phosphorylates myosin light chain kinase (MLCK), which leads to decrease in myosin light chain phosphorylation levels.[15] PKA also phosphorylates G protein-coupled receptor kinase 2 and regulator of G protein signaling proteins, enhancing the inactivation of $G\alpha_q$-mediated signaling in VSMCs and resulting in suppression of agonist-induced vasoconstriction.[16–18] Thus, the phosphorylation of these targets can explain the mechanism of PKA-dependent vasodilation. However, it is still unclear why cilostazol induces a decrease in $[Ca^{2+}]_i$ of VSMCs through PKA activation.

The transient receptor potential channel was originally identified in a *Drosophila* visual transduction mutation, *trp*, in which the receptor potential is transient on light perception.[19] The canonical subfamily transient receptor potential canonical (TRPC) channels are thought as putative candidates for receptor-operated cation channels (ROCCs).[20] Among the 7 members of vertebrate TRPCs (TRPC1 to TRPC7), TRPC2, TRPC3, TRPC6, and TRPC7 have been reported to be activated by DAG.[21,22] Sustained cation influx induced by activation of DAG-activated TRPC channels leads to membrane depolarization, resulting in increase of $[Ca^{2+}]_i$ through activation of voltage-dependent L-type Ca^{2+} channels (VDCCs).[22,23] In addition, DAG-activated TRPC channels associate with the Na^+/Ca^{2+} exchanger, and TRPC-mediated Na^+ influx results in a shift of Na^+/Ca^{2+} exchanger operation to the reverse mode (ie, Ca^{2+} influx).[24,25] The resultant Ca^{2+} influx mediated by DAG-activated cation influx through TRPC channels are required for muscle contraction[7,8] and gene expression.[23,26]

The activity of DAG-activated TRPC channels is negatively regulated by their phosphorylation.[27–30] Protein kinase C has been implicated in the suppression of TRPC3 channel activity via phosphorylation of human TRPC3 at Ser712, and protein kinase G (PKG)-dependent phosphorylation has been shown to suppress store-operated Ca^{2+} entry in TRPC3-expressing HEK293 cells through phosphorylation of human TRPC3 at Thr11 and Ser263.[27–29] In addition, PKG-dependent phosphorylation of rodent TRPC6 at Thr69 has been shown to mediate nitric oxide-dependent reduction of TRPC6 channel activity in VSMCs.[30] As the inhibition of TRPC6 reduces agonist-induced membrane depolarization in VSMCs, the nitric oxide-mediated inhibition of TRPC6 channels may be partially involved in the mechanism of endothelium-dependent vasodilation. Activation of PKA by stimulation of the β_2 adrenergic receptor or inhibition of PDE3 is known to induce endothelium-independent vascular relaxation. However, it is unknown whether activation of PKA suppresses vasoconstriction through inhibition of TRPC channels.

In this study, we demonstrated that PKA-mediated phosphorylation of TRPC6 channels at Thr69 underlies suppression of agonist-induced contraction of aortic VSMCs by PDE3 inhibition. We further demonstrated the molecular mechanism underlying selective phosphorylation of TRPC6 at Thr69 by PDE3 inhibition in rat aortic smooth muscle cells (RAoSMCs).

Methods

The supplemental materials (available online at http://atvb.ahajournals.org) provide expanded descriptions.

Isometric Force Measurements

Rats were anesthetized with sodium pentobarbital (50 mg/kg IP), and the descending thoracic aorta was carefully isolated and cut into 3-mm-long rings. The rings were stretched to a resting tension of 1.5*g*. We confirmed that pretreatment with PDE3 inhibitors did not affect the resting tension.

Measurement of $[Ca^{2+}]_i$ and Rho Activity, Electrophysiology, Immunoprecipitation, and Western Blot Analyses

Measurement of $[Ca^{2+}]_i$ and Rho activity, patch clamp recording of HEK293 cells, immunoprecipitation of green fluorescent protein (GFP)-fused proteins, and Western blot analyses were performed as described previously.[30,31,32]

Production of a Reconstituted Ring and Measurement of Tension

Production of a reconstituted ring and measurement of tension were performed as described previously.[33] The cultured primary RAoSMCs were collected with trypsinization and transfected with pCIneo vector encoding wild-type TRPC6 or TRPC6-Thr69Ala mutant and pEGFP-N1 using electroporation (1400 V, 10 ms×3, Digital-Bio). Cell suspensions were mixed with the culture medium (5×10^6 cells/mL) containing 0.6 mg/mL type I collagen (Cellmatrix Type I-P). The mixture (100 μL, 0.5×10^6 cells) was placed around a silicone column (ϕ=2 mm), which was attached on the center of the silicone disc (ϕ=8 mm). After the collagen gel became solid, the culture medium was added and cultured for 24 to 48 hours. The ring preparation thus obtained was used for measurements of isometric tension development. The transfection efficiency of electroporation was 70±5%, determined by counting GFP-positive RAoSMCs. Tension recordings are described in the supplemental materials.

Statistical Analysis

The results are shown as mean±SEM. All experiments were repeated at least 3 times. Statistical comparisons were made with the 2-tailed Student *t* test or analysis of variance followed by the Student-Newman-Keuls procedure, with significance imparted at probability values <0.05.

Results

Suppression of Agonist-Induced Vasoconstriction by PDE3 Inhibition

Treatment of rat thoracic aorta with G_q protein-coupled receptor agonists (angiotensin II [Ang II], phenylephrine, and U46619) increased the tension of aortic rings, which was significantly suppressed by pretreatment with cilostazol in a concentration-dependent manner (Figure 1A to 1C). Cilostazol suppressed vasoconstriction induced by Ang II more selectively than phenylephrine and U46619. Cilostazol did not suppress KCl-induced contraction (Figure 1D), indicating that cilostazol does not inhibit voltage-dependent Ca^{2+} channels. In addition, the Ang II–induced contraction was markedly reduced by the removal of extracellular Ca^{2+}, and the effects of cilostazol were abolished in extracellular Ca^{2+}-free solution (Figure 1E and 1F). Cilostazol-induced suppression of Ang II contraction in Ca^{2+}-containing solution was not affected by the removal of endothelium (Figure 1G). Milrinone, another PDE3-selective inhibitor, also suppressed Ang II–induced contraction (Supplemental Figure I). These results suggest that PDE3 inhibition suppresses agonist-induced Ca^{2+} influx in aortic smooth muscle cells. The Ang II–induced contraction was completely suppressed by CV11974, an Ang II type 1 receptor antagonist (Figure 1H). Further-

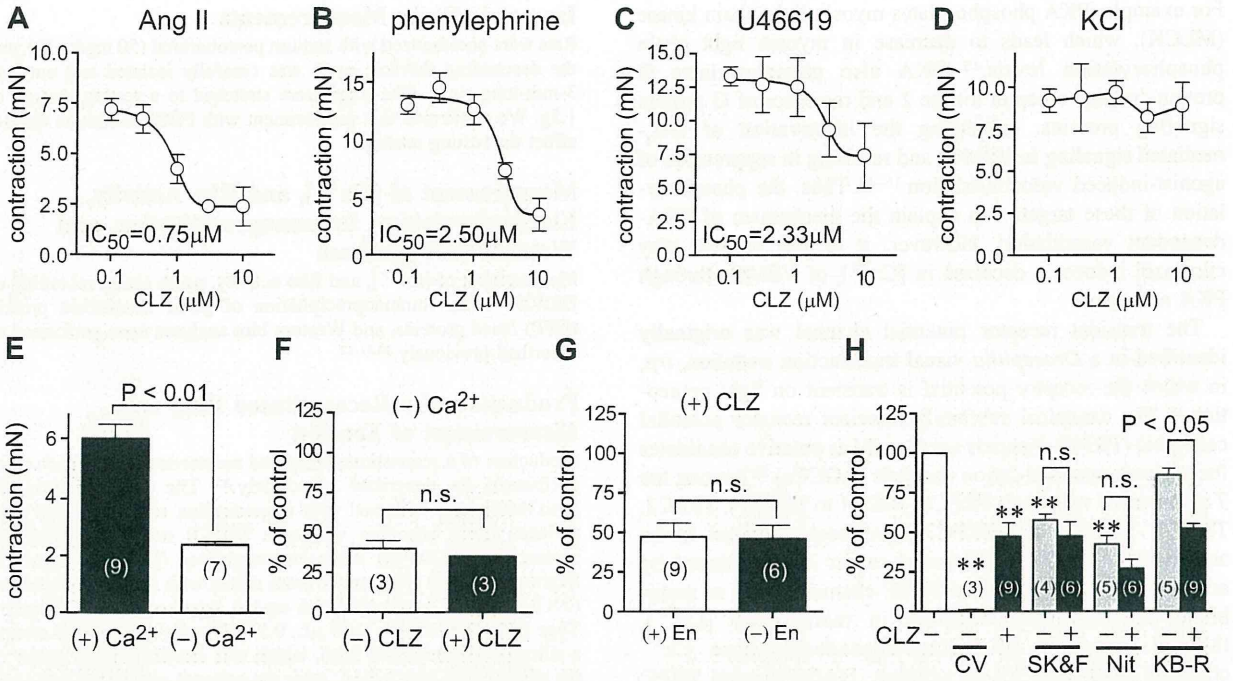

Figure 1. Inhibition of phosphodiesterase (PDE) 3 suppresses agonist-induced vascular contraction in rat thoracic aorta. A to D, Concentration-dependent inhibition of agonist-induced vasoconstriction by cilostazol (CLZ). Vascular contraction was induced by 100 nmol/L angiotensin II (Ang II) (A), 1 μmol/L phenylephrine (B), 100 nmol/L U46619 (C), and 40 mmol/L KCl (D). Aorta was pretreated with CLZ for 30 minutes before agonist stimulation. E, Requirement of extracellular Ca^{2+} in Ang II–induced vasoconstriction. F, Effects of CLZ on Ang II–induced contraction in the absence of extracellular Ca^{2+}. G, Suppression of Ang II–induced contraction by CLZ treatment in endothelium (En)-denuded aorta. H, Ang II–induced contraction in the aortas pretreated with SK&F96365 (SK&F; 7 μmol/L), nitrendipine (Nit; 3 μmol/L), and KB-R7943 (KB-R; 5 μmol/L) with or without CLZ (5 μmol/L) for 30 minutes before Ang II stimulation. $^{**}P<0.01$ vs control (white column). n.s. indicates not significant.

more, the suppression of Ang II–induced contraction by cilostazol was abolished by inhibitors of ROCCs (SK&F96365) and VDCCs (nitrendipine) but not by an Na^+/Ca^{2+} exchanger (KB-R7943). As activation of ROCCs reportedly induces membrane depolarization,[23,34] these results suggest that PDE3 inhibition suppresses agonist-induced Ca^{2+} influx through VDCCs by inhibiting ROCCs.

Cilostazol Inhibits DAG-Activated TRPC Channels

TRPC channels are believed to be a molecular candidate of ROCCs.[20] Among 7 TRPC homologues, TRPC3, TRPC6, and TRPC7 proteins (TRPC3/6/7) are expressed in aorta and function as a DAG-activated cation channels in VSMCs.[35] Cilostazol did not affect ATP-induced Ca^{2+} release from the intracellular Ca^{2+} store but significantly suppressed Ca^{2+} influx–mediated increases in $[Ca^{2+}]_i$ in TRPC3-, TRPC6-, or TRPC7-expressing HEK293 cells (Figure 2). The IC_{50} values of inhibition by cilostazol were 0.75±0.06 μmol/L (for TRPC3), 0.73±0.24 μmol/L (for TRPC6), and 0.71±0.04 μmol/L (for TRPC7). Cilostazol also suppressed Ca^{2+} influx–mediated increases in $[Ca^{2+}]_i$ induced by 1-oleoyl-2-acetyl-*sn*-glycerol (OAG) in TRPC3-, TRPC6-, or TRPC7-expressing cells, with IC_{50} values being 0.61±0.19, 0.68±0.18, and 0.69±0.22 μmol/L, respectively (Supplemental Figure II). However, ATP-induced Ca^{2+} influx through TRPC5 channels, which is believed to be insensitive to DAG, and store-operated Ca^{2+} influx induced by ionomycin were not suppressed by cilostazol (Supplemental Figure III). These results suggest that inhibition of PDE3 specifically suppresses agonist-induced Ca^{2+} influx through DAG-activated TRPC channels.

Involvement of Phosphorylation of TRPC6 at Thr69 in Suppression of TRPC6 Channel Activity by PDE3 Inhibition

As more than 15 minutes of pretreatment with cilostazol was required for the significant suppression of TRPC6-mediated Ca^{2+} influx induced by ATP or OAG (Supplemental Figure IV), cilostazol may not directly inhibit TRPC6 channel activity. In addition, localization of GFP-fused TRPC3 (TRPC3-GFP) and TRPC6 (TRPC6-GFP) proteins on the plasma membrane were not affected by cilostazol treatment (Supplemental Figure V). These results suggest that PDE3 inhibition did not change the membrane localization of TRPC proteins. Takahashi et al has reported that PKG-dependent phosphorylation of TRPC6 at Thr69 suppresses TRPC6 channel activity.[30] As PKA and PKG recognize a similar substrate sequence,[36] we next examined the involvement of TRPC6 phosphorylation at Thr69 in suppression of TRPC6 channel activity by PDE3 inhibition. The Ca^{2+} influx–mediated $[Ca^{2+}]_i$ increase induced by OAG was suppressed by cilostazol pretreatment in wild-type TRPC6 (TRPC6-wt)-expressing cells, whereas the suppression of OAG-mediated Ca^{2+} influx by cilostazol was completely abolished in TRPC6-Thr69Ala-expressing cells (Supplemental Figure VI). The inhibition of TRPC6-mediated Ca^{2+} influx by cilostazol

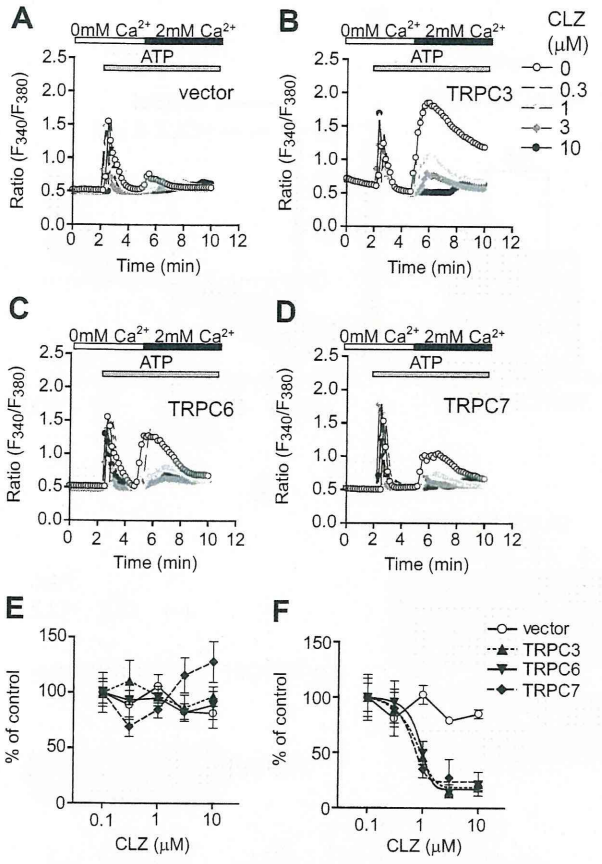

Figure 2. Suppression by phosphodiesterase (PDE) 3 inhibition of agonist-induced Ca^{2+} influx mediated by diacylglycerol (DAG)-activated transient receptor potential canonical (TRPC) channels. A to D, Average time courses of ATP-stimulated changes in intracellular Ca^{2+} concentration ($[Ca^{2+}]_i$) determined by Fura-2 ratio (Ratio) in vector-, TRPC3-, TRPC6-, and TRPC7-overexpressing HEK293 cells. Ca^{2+} release–mediated $[Ca^{2+}]_i$ increase was first induced by ATP (100 μmol/L) in Ca^{2+}-free external solution, and then Ca^{2+} influx–mediated $[Ca^{2+}]_i$ increase was induced by the addition of Ca^{2+} (2 mmol/L). Cells were pretreated with the indicated concentration of cilostazol (CLZ) for 30 minutes before ATP stimulation. E and F, Peak changes in intracellular Ca^{2+} concentration induced by ATP in the absence (E) or presence (F) of extracellular Ca^{2+}. n=48 to 74 cells.

was also abolished by cotreatment with KT5720, a PKA inhibitor, but not by KT5823 (a PKG inhibitor) or Go6976 (a protein kinase C inhibitor) (Supplemental Figure VII). In addition, treatment with 8-Br-cAMP and forskolin significantly suppressed Ca^{2+} influx–mediated $[Ca^{2+}]_i$ increases induced by OAG stimulation in TRPC6-wt-expressing cells, whereas both PKA activators did not suppress OAG-induced $[Ca^{2+}]_i$ increases in TRPC6-Thr69Ala-expressing cells (Supplemental Figure VI). Furthermore, stimulation of muscarinic receptor with carbachol induced inward currents in TRPC6-wt-expressing cells; these currents were completely suppressed by the pretreatment with cilostazol (Figure 3A to 3C). The suppression of TRPC6-induced currents by cilostazol was abolished in cells expressing TRPC6-Thr69Ala (Figure 3D). These results suggest that PKA-dependent phosphorylation of TRPC6 at Thr69 underlies inhibition of TRPC6 channel activity by PDE3 inhibition.

PKA-Dependent Phosphorylation of TRPC6 by PDE3 Inhibition

We have recently generated an anti-phospho-TRPC6 (Thr69) antibody[37] and found that activation of PKA by the treatment with forskolin and cilostazol dramatically increased the phosphorylation of TRPC6 at Thr69 in TRPC6-wt-expressing cells, which was not observed in TRPC6-Thr69Ala-expressing cells (Figure 3E). This result suggests the specific recognition of Thr69 phosphorylation by this antibody. Treatment of HEK293 cells with cilostazol increased TRPC6 phosphorylation levels ≈1.5-fold, which was completely suppressed by cotreatment with KT5720. Treatment with cilostazol gradually increased TRPC6 phosphorylation levels (Figure 3F). The time course of this phosphorylation was consistent with the time of pretreatment required to obtain the inhibition of TRPC6-mediated Ca^{2+} influx with cilostazol (Supplemental Figure IV). Although cilostazol completely suppressed TRPC6-mediated Ca^{2+} influx, as in the case of forskolin (Supplemental Figure VI), the extent of TRPC6 phosphorylation by cilostazol was much weaker than that by forskolin. However, phosphorylation levels of membrane-localized TRPC6 proteins induced by cilostazol were similar to those induced by forskolin (Figure 3G). These results suggest that phosphorylation of plasma membrane-localized TRPC6 proteins is essential for suppression of TRPC6 channel activity by PDE3 inhibition.

Phosphorylation of TRPC6 at Thr69 Is Essential for Suppression of Ang II–Induced Ca^{2+} Influx by PDE3 Inhibition in RAoSMCs

We next examined which endogenous TRPC subtype(s) is involved in Ang II–induced Ca^{2+} influx in RAoSMCs. Although Ang II–induced Ca^{2+} release was not suppressed by the knockdown of TRPC3/6/7, the Ca^{2+}-influx-mediated Ca^{2+} response induced by Ang II was suppressed by knockdown of TRPC6 but not of TRPC3 and TRPC7 (Figure 4A and 4B). Pretreatment with cilostazol significantly reduced Ca^{2+} influx–mediated Ca^{2+} responses induced by Ang II, which was abolished by TRPC6 knockdown. We found that TRPC3 and TRPC6 proteins were actually expressed in RAoSMCs, and expression levels of TRPC proteins were actually suppressed by siRNA treatment (Figure 4C). Human TRPC3 has 2 sites (Thr11 and Ser263) phosphorylated by PKG or PKA, and Ser263 (position 2), but not Thr11 (position 1), is conserved in rodent TRPC3/6/7 proteins (Supplemental Figure VI). As the expression of mouse TRPC3 mutant (Ser251Ala) abolished the suppression of OAG-induced Ca^{2+} response by cilostazol, position 2 may be involved in suppression of TRPC3 channel activity by PDE3 inhibition. However, pretreatment of RAoSMCs with cilostazol actually induced phosphorylation of TRPC6 at Thr69 (position 1) but did not induce phosphorylation of TRPC3/6/7 at Ser (position 2), although forskolin cotreatment induced phosphorylation of these sites (Figure 4D). These results suggest that PDE3 inhibition suppresses Ang II–induced Ca^{2+} influx via local PKA-mediated phosphorylation of TRPC6 at Thr69 in RAoSMCs.

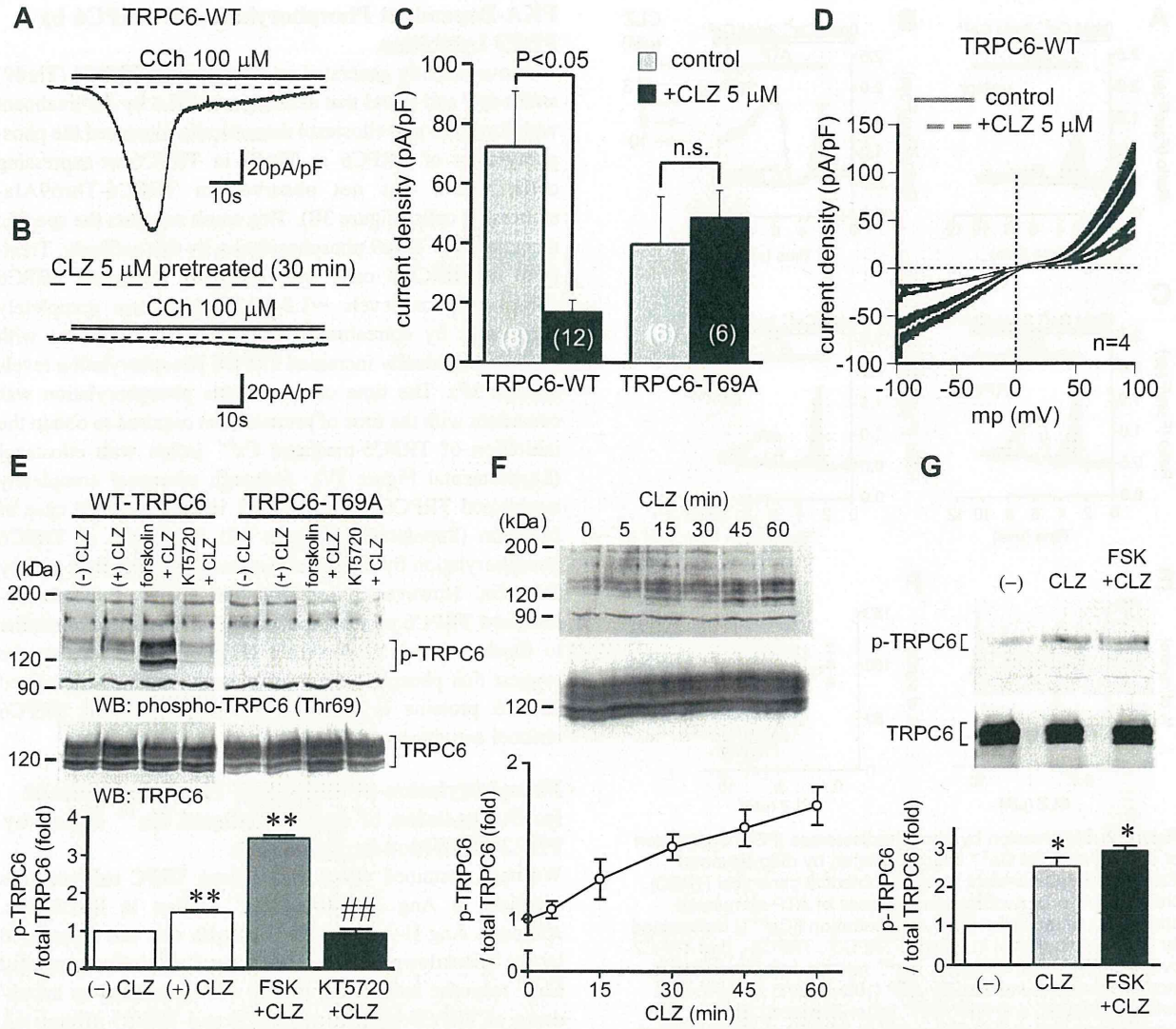

Figure 3. Requirement of phosphorylation of transient receptor potential canonical (TRPC) 6 at Thr69 in suppression of TRPC6 currents by phosphodiesterase (PDE) 3 inhibition. A and B, Typical traces of inward cation currents induced by carbachol (CCh; 100 μmol/L)) without (A) or with (B) cilostazol (CLZ) pretreatment. Cells were pretreated with CLZ (5 μmol/L) for 30 minutes before addition of CCh. WT indicates wild-type. C, Average TRPC6-induced current density at the holding potential of −50 mV with or without CLZ pretreatment in TRPC6-wt- and TRPC6-Thr69Ala-expressing cells. Numbers of experiments are shown in the columns. n.s. indicates not significant. D, Current-voltage relationship of wild-type and Thr69Ala-mutated TRPC6 channels with or without pretreatment with CLZ. To construct the latter, rising voltage ramps (−100 to +100 mV, 2 s) were applied. E, Effects of forskolin (FSK) and KT5720 on CLZ-induced TRPC6 phosphorylation in TRPC6-wt- and TRPC6-Thr69Ala-overexpressing cells. Cells were treated with CLZ (5 μmol/L), forskolin (10 μmol/L), and KT5720 (0.1 μmol/L) for 30 minutes. F, Time courses of TRPC6 phosphorylation induced by CLZ (5 μmol/L) in TRPC6-expressing HEK293 cells. G, Effects of forskolin on CLZ-induced phosphorylation of TRPC6 proteins expressed in the plasma membrane. n=3 experiments. *$P<0.05$, **$P<0.01$ vs control (−), ##$P<0.01$ vs CLZ.

Formation of the TRPC-PKA-PDE3 Signal Complex in the Plasma Membrane

We further examined whether DAG-activated TRPC channels functionally interact with PKA and PDE3. TRPC3-GFP, TRPC6-GFP, and farnesylation signal-encoding GFP proteins are predominantly expressed in crude membrane fraction of HEK293 cells, whereas PKA is predominantly expressed in cytosol. Immunoprecipitation of GFP-containing proteins revealed that endogenous PDE3A could associate with TRPC3-GFP and TRPC6-GFP but not with farnesylation signal-encoding GFP proteins. In addition, PKA catalytic subunit also associated with TRPC3-GFP and TRPC6-GFP (Figure 5A). Treatment with cilostazol actually induced phosphorylation of TRPC3/6/7 at Ser (position 2) (Figure 5B). These results suggest that TRPC3/6/7 could form a signal complex with PDE3 and PKA beneath the plasma membrane in HEK293 cells. However, endogenous TRPC6 associated with PDE3A and PKA more potently than TRPC3 in RAoSMCs (Figure 5C), suggesting that endogenous TRPC6 preferentially forms a ternary complex with PDE3 and PKA in RAoSMCs.

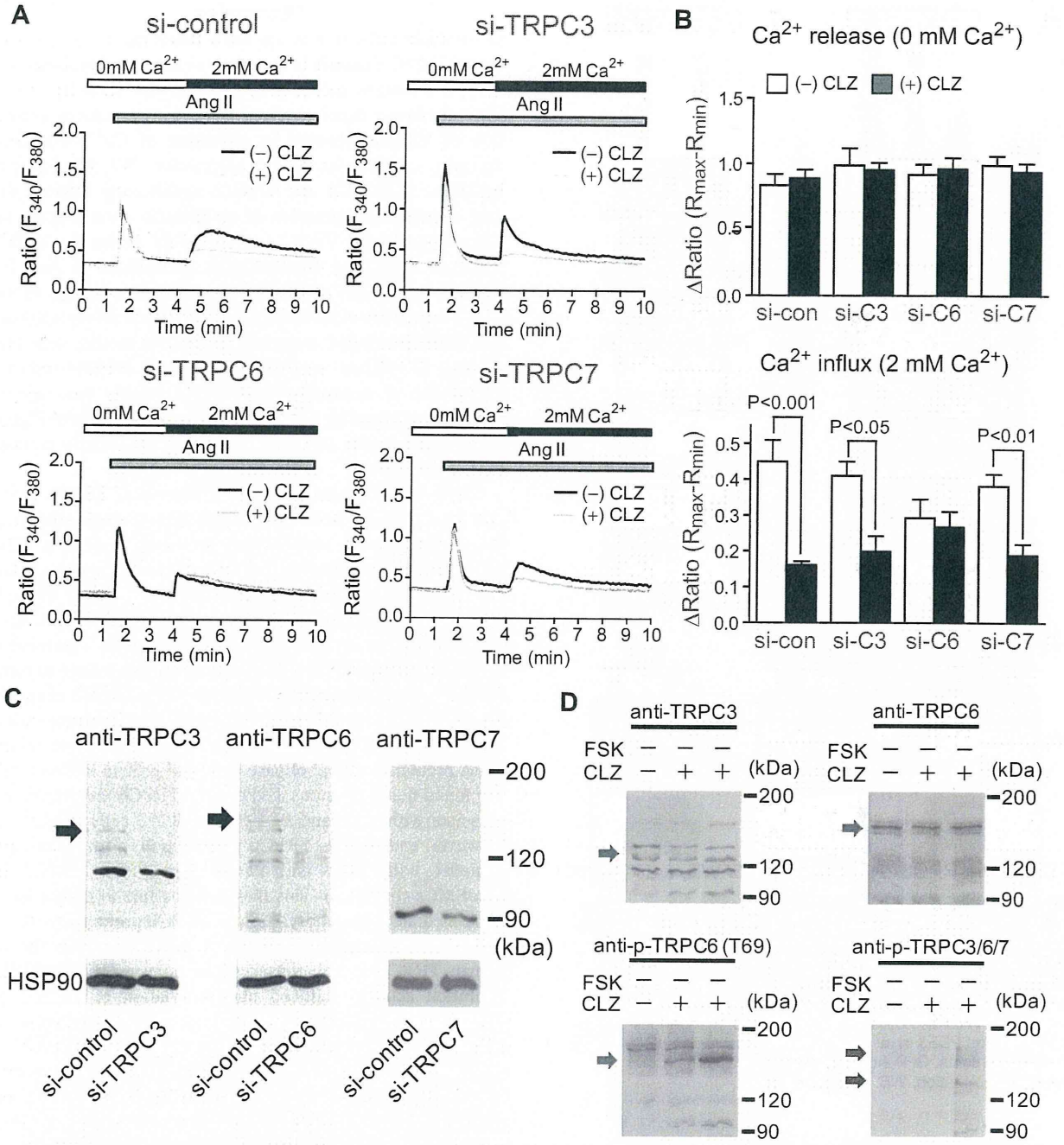

Figure 4. Requirement of transient receptor potential canonical (TRPC) 6 phosphorylation in the suppression of angiotensin II (Ang II)–induced Ca^{2+} influx by phosphodiesterase (PDE) 3 inhibition in rat aortic smooth muscle cells (RAoSMCs). A and B, Average time courses of Ca^{2+} responses (A) and peak $[Ca^{2+}]_i$ increases induced by Ang II (100 nmol/L) (B) in the presence or absence of cilostazol (CLZ) (1 μmol/L) in RAoSMCs treated with small interfering (si) RNAs for control or TRPC3, TRPC6, or TRPC7. n=24 to 38 cells. C, Expression levels of native TRPC proteins in respective TRPC-knocked-down RAoSMCs. D, Phosphorylation of TRPC6 but not TRPC3 and TRPC7 by CLZ (10 μmol/L) with or without forskolin (FSK) (30 μmol/L) for 1 hour. n=3 experiments.

Requirement of TRPC6 Phosphorylation for Cilostazol-Induced Suppression of Vasoconstriction Induced by Ang II in VSMC

To examine the functional relevance of TRPC6 phosphorylation at Thr69 to the vasodilating effect of cilostazol, we examined the effects of TRPC6-Thr69Ala in RAoSMCs. Treatment of RAoSMCs with Ang II induced a transient increase in $[Ca^{2+}]_i$, which was significantly suppressed by pretreatment with cilostazol (Figure 6A and 6B). Overexpression of TRPC6-wt slightly enhanced the Ang II–induced Ca^{2+} response, which was also suppressed by cilostazol. In contrast, overexpression of TRPC6-Thr69Ala abolished the suppression of Ang II–induced Ca^{2+} response by cilostazol pretreatment. We next examined the contractile response

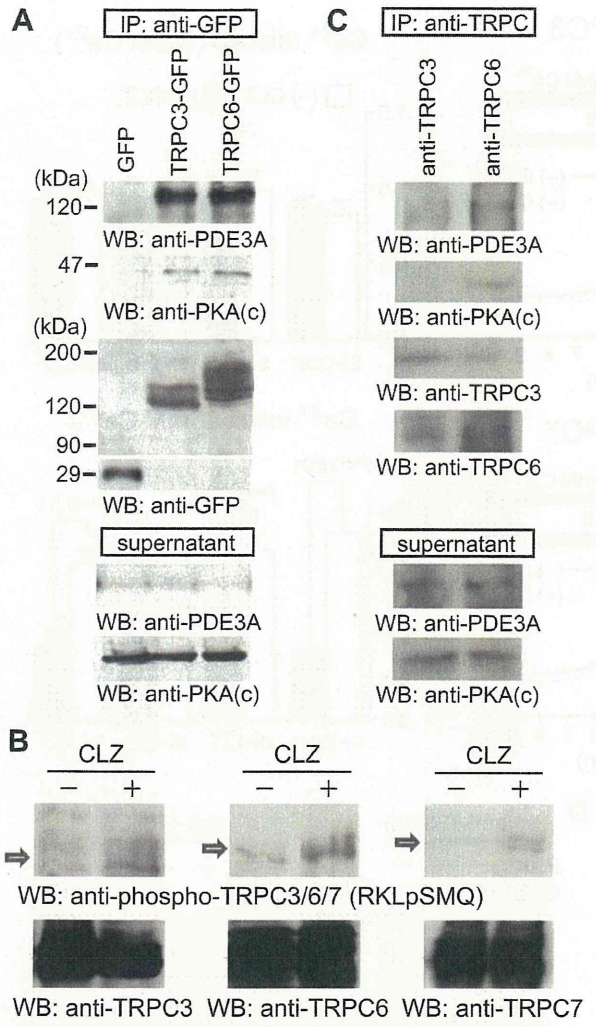

Figure 5. Association of transient receptor potential canonical (TRPC) channels with protein kinase A (PKA) and phosphodiesterase (PDE) 3 proteins. A, Interaction of TRPC proteins with PKA catalytic subunit and PDE3A in vector-, TRPC3-, and TRPC6-overexpressing HEK293 cells. B, Phosphorylation of TRPC proteins by the treatment with cilostazol (CLZ) (10 μmol/L) for 1 hour in HEK293 cells. C, Association of endogenous TRPC6 with PKA and PDE3 in rat aortic smooth muscle cells (RAoSMCs). n=3 experiments. GFP indicates green fluorescent protein; IP, immunoprecipitation; WB, Western blotting.

of the aortic rings reconstituted from RAoSMCs. Treatment of reconstituted aortic ring with Ang II induced contraction, which was significantly attenuated by pretreatment with cilostazol in the vector (GFP)-expressing rings (Figure 6C and 6D). In contrast, the expression of TRPC6-Thr69Ala abolished the suppression of Ang II–induced contraction by cilostazol pretreatment. A dominant-negative mutant of TRPC6 (TRPC6-3A) also abolished the cilostazol-induced suppression of Ang II–induced contraction (Supplemental Figure VIII). These results suggest that the phosphorylation of TRPC6 at Thr69 is required for the suppression of Ang II–induced contraction by cilostazol in RAoSMCs.

Discussion

In excitable cells, one of the main functions of receptor-activated TRPC channels is to induce membrane depolarization through sustained cation influx by receptor stimulation.[23,34] The membrane depolarization subsequently induces activation of VDCCs, leading to activation of Ca^{2+}-dependent signaling required for muscle contraction. We revealed that inhibition of ROCCs and VDCCs significantly reduced the Ang II–induced contraction of rat thoracic aorta (Figure 1), suggesting that the VDCC-mediated Ca^{2+} influx via TRPC-mediated membrane depolarization is involved in Ang II–induced contraction of rat thoracic aorta. In contrast, as the magnitude of the suppression by cilostazol of phenylephrine- and U46619-induced vasoconstriction was smaller than that of Ang II–induced vasoconstriction, and U46619-induced contraction of reconstituted rings was weakly (not significantly) suppressed by PDE3 inhibition (Supplemental Figure VIII). These results suggest that Ang II preferentially induces DAG-mediated Ca^{2+} influx in aortic VSMCs.

We have shown the critical involvement of TRPC6 channels in Ang II–induced vasoconstriction through analyzing the mechanism of vasodilation by PDE3 inhibition. The PDE3 inhibition specifically suppresses DAG-mediated (but not IP_3-mediated and store-operated) Ca^{2+} influx through PKA-dependent phosphorylation of TRPC3/6/7. TRPC proteins are known to function not only as a Ca^{2+}-permeable channel-forming subunit but also as a scaffold protein to form the Ca^{2+} signaling complex.[38] For example, TRPC3 channels are reported to associate with several signaling molecules, such as IP_3 receptors, calmodulin, vesicle-associated membrane protein 2, phospholipase C-γ, and protein kinase C.[9,31] We found that exogenous TRPC3 and TRPC6 proteins could associate with PKA and PDE3 in HEK293 cells (Figure 5). However, endogenous TRPC6 preferentially forms a ternary complex with PKA and PDE3 rather than TRPC3 in RAoSMCs (Figure 5). This makes it possible to induce local PKA-mediated phosphorylation of TRPC6 proteins by PDE3 inhibition. Although the position 1 phosphorylation site of human TRPC3 is not conserved in mouse TRPC3, PDE3 inhibition actually induced phosphorylation of TRPC3 at Ser251 and of TRPC7 at Ser267 (Figure 5). As the inhibition of TRPC3 phosphorylation canceled suppression of TRPC3-mediated Ca^{2+} influx by PDE3 inhibition (Supplemental Figure VI), our results indicate that the PKG phosphorylation sites of DAG-activated TRPC channels are also targets of PKA.

It has been thought that phosphorylation of MLCK is essential for the PKA-mediated vasodilating action.[39] However, the present results suggest that PKA induces vasodilation through 2 mechanisms: one is to suppress agonist-induced Ca^{2+} influx through inhibition of DAG-activated TRPC channels, and the other is to inhibit MLCK activity by phosphorylation of MLCK. As PDE3 inhibition did not suppress the KCl-induced contraction, PKA-mediated inhibition of MLCK activity may not participate in the vasodilating effects of PDE3 inhibition. In addition, Rho functions as an essential mediator in agonist-induced vasoconstriction.[33,39] Rho decreases myosin light chain phosphatase activity through Rho kinase-mediated phosphorylation. It has been reported that TRPC6-mediated Ca^{2+} influx induces RhoA

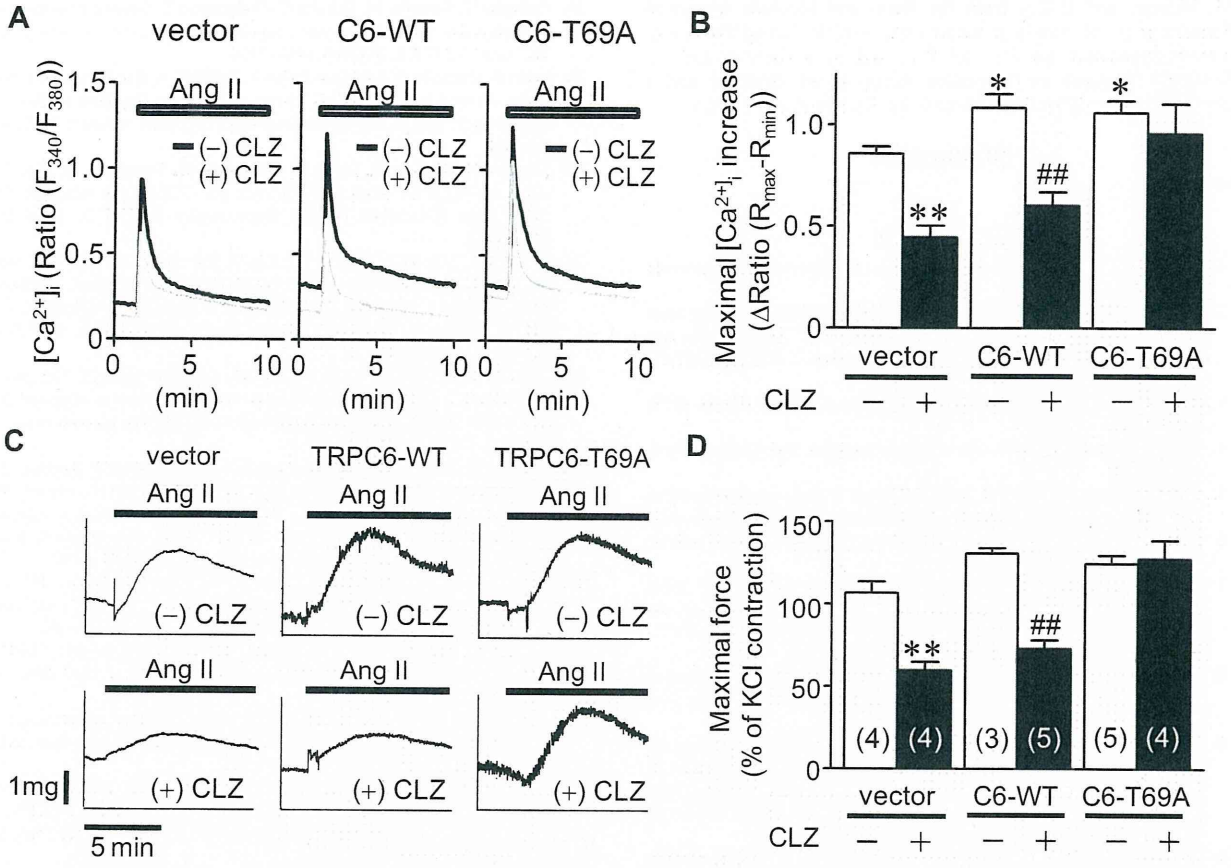

Figure 6. Requirement of transient receptor potential canonical (TRPC) 6 phosphorylation in the suppression of angiotensin II (Ang II)–induced aortic contraction by phosphodiesterase (PDE) 3 inhibition. A, Effects of cilostazol (CLZ) on Ang II–induced Ca^{2+} responses in primary cultured rat aortic smooth muscle cells (RAoSMCs) expressing vector (pcDNA3), TRPC6-wild-type (wt), or TRPC6-Thr69Ala. Cells were treated with CLZ for 30 minutes before addition of Ang II (100 nmol/L). B, Peak increase in $[Ca^{2+}]_i$ induced by Ang II (100 nmol/L) in the presence or absence of CLZ (10 μmol/L). n=40 to 80 cells. C, Representative time courses of changes in tensions of aortic ring reconstituted from RAoSMCs expressing vector, TRPC6-wt, TRPC6-Thr69Ala, or dominant-negative mutant of TRPC6 (TRPC6-3A). CLZ (10 μmol/L) was treated for 30 minutes before stimulation with Ang II (100 nmol/L). D, Peak contraction induced by Ang II in the absence (−) or presence (+) of CLZ. *P<0.05, **P<0.01 vs (−) CLZ, ##P<0.01 vs C6-wild-type (WT) (−) CLZ.

activation in thrombin-stimulated endothelial cells.[40] However, PDE3 inhibition did not attenuate agonist-induced Rho activation in RAoSMCs (Supplemental Figure VIII). Thus, PDE3 inhibition may not affect the Rho-mediated signaling pathway.

Cilostazol has many pharmacological actions, including vasodilation, inhibition of platelet activation and aggregation, inhibition of thrombosis, increased blood flow to the limbs, improvement in serum lipids with lowering of triglycerides and elevation of high-density lipoprotein cholesterol, and inhibition of growth of VSMCs.[10–12] Nakamura et al have previously reported the PKA-independent vasodilating effect of PDE3 inhibition using pressurized rabbit cerebral penetrating arterioles.[41] It is expected that the effectiveness of vasodilation by PDE3 inhibition is greatly dependent on the kinds of blood vessel sampled, the agonist stimulation, and the timing of drug treatment. Thus, our present study is only to show a novel mechanism underlying PKA-dependent vasodilation by PDE3 inhibition. Cilostazol is clinically applicable to the patients with intermittent claudication and arteriosclerosis obliteration.[10–12] It is generally thought that endothelium-dependent vasodilation and capillary-like formation underlies protection of PDE3 inhibition against peripheral arterial disease. Although the relationship between TRPC channels and peripheral arterial disease is still unknown, our findings will provide a novel mechanism underlying endothelium-independent improvement of peripheral blood flow by PDE3 inhibition.

In conclusion, we demonstrated that PDE3 inhibition specifically suppresses DAG-mediated Ca^{2+} influx through PKA-dependent phosphorylation of TRPC3/6/7 channels in HEK293 cells. Furthermore, DAG-activated TRPC6 channels were found to mediate the Ang II–induced contraction of aortic VSMCs, and PDE3 inhibition preferentially induced phosphorylation of rodent TRPC6 at Thr69. Formation of TRPC6/PDE3/PKA ternary complex may be involved in this mechanism. These findings will indicate the novel mechanism underlying the vasorelaxant effects of PDE3 inhibition against vasoactive hormones.

Sources of Funding

This study was supported by grants from the Ministry of Education, Culture, Sports, Science, and Technology of Japan (to M. Nishida,

M. Nakaya, and H.K.); from the Naito and Mochida Memorial Foundation (to M. Nishida); and from the Vehicle Racing Commemorative Foundation (to T.I. and R.I.) and by a Grant-in-Aid for Scientific Research on Innovative Areas (to M. Nishida) and a Grant-in-Aid for Scientific Research on Priority Areas (H.K.).

Disclosures

None.

References

1. Johnson PC. The myogenic response and the microcirculation. *Microvasc Res*. 1977;13:1–18.
2. Akata T. Cellular and molecular mechanisms regulating vascular tone: part 1: basic mechanisms controlling cytosolic Ca^{2+} concentration and the Ca^{2+}-dependent regulation of vascular tone. *J Anesth*. 2007;21:220–231.
3. Berridge MJ. Inositol trisphosphate and calcium signalling. *Nature*. 1993;361:315–325.
4. Putney JW Jr. Capacitative calcium entry revisited. *Cell Calcium* 1990;11:611–624.
5. Leung FP, Yung LM, Yao X, Laher I, Huang Y. Store-operated calcium entry in vascular smooth muscle. *Brit J Pharmacol*. 2008;153:846–857.
6. Nishizuka Y. Protein kinase C and lipid signaling for sustained cellular responses. *FASEB J*. 1995;9:484–496.
7. Inoue R, Okada T, Onoue H, Hara Y, Shimizu S, Naitoh S, Ito Y, Mori Y. The transient receptor potential protein homologue TRP6 is the essential component of vascular α1-adrenoceptor-activated Ca^{2+}-permeable cation channel. *Circ Res*. 2001;88:325–332.
8. Welsh DG, Morielli AD, Nelson MT, Brayden JE. Transient receptor potential channels regulate myogenic tone of resistance arteries. *Circ Res*. 2002;90:248–250.
9. Dietrich A, Mederos Y Schnitzler M, Gollasch M, Gross V, Storch U, Dubrovska G, Obst M, Yildirim E, Salanova B, Kalwa H, Essin K, Pinkenburg O, Luft FC, Gudermann T, Birnbaumer L. Increased vascular smooth muscle contractility in $TRPC6^{-/-}$ mice. *Mol Cell Biol*. 2005;25:6980–6989.
10. Kimura Y, Tani T, Kanbe T, Watanabe K. Effect of cilostazol on platelet aggregation and experimental thrombosis. *Arzneimittelforschung*. 1985;35(7A):1144–1149.
11. Kambayashi J, Liu Y, Sun B, Shakur Y, Yoshitake M, Czerwiec F. Cilostazol as a unique antithrombotic agent. *Curr Pharm Des*. 2003;9:2289–2302.
12. Dawson DL, Cutler BS, Meissner MH, Strandness DE, Jr. Cilostazol has beneficial effects in treatment of intermittent claudication: results from a multicenter, randomized, prospective, double-blind trial. *Circulation*. 1998;98:678–686.
13. Tanaka T, Ishikawa T, Hagiwara M, Onoda K, Itoh H, Hidaka H. Effects of cilostazol, a selective cAMP phosphodiesterase inhibitor on the contraction of vascular smooth muscle. *Pharmacology*. 1988;36:313–320.
14. Shiraishi Y, Kanmura Y, Itoh T. Effect of cilostazol, a phosphodiesterase type III inhibitor, on histamine-induced increase in $[Ca^{2+}]_i$ and force in middle cerebral artery of the rabbit. *Brit J Pharmacol*. 1998;123:869–878.
15. Adelstein RS, Conti MA, Hathaway DR, Klee CB. Phosphorylation of smooth muscle myosin light chain kinase by the catalytic subunit of adenosine 3′: 5′-monophosphate-dependent protein kinase. *J Biol Chem*. 1978;253:8347–8350.
16. Huang J, Zhou H, Mahavadi S, Sriwai W, Murthy KS. Inhibition of $G\alpha_q$-dependent PLC-β1 activity by PKG and PKA is mediated by phosphorylation of RGS4 and GRK2. *Am J Physiol Cell Physiol*. 2007;292:C200–C208.
17. Heximer SP, Knutsen RH, Sun X, Kaltenbronn KM, Rhee MH, Peng N, Oliveira-dos-Santos A, Penninger JM, Muslin AJ, Steinberg TH, Wyss JM, Mecham RP, Blumer KJ. Hypertension and prolonged vasoconstrictor signaling in RGS2-deficient mice. *J Clin Invest*. 2003;111:445–452.
18. Harris DM, Cohn HI, Pesant S, Eckhart AD. GPCR signalling in hypertension: role of GRKs. *Clin Sci (Lond)*. 2008;115:79–89.
19. Montell C, Rubin GM. Molecular characterization of the *Drosophila trp* locus: a putative integral membrane protein required for phototransduction. *Neuron*. 1989;2:1313–1323.
20. Nishida M, Hara Y, Yoshida T, Inoue R, Mori Y. TRP channels: molecular diversity and physiological function. *Microcirculation*. 2006;13:535–550.
21. Hofmann T, Schaefer M, Schultz G, Gudermann T. Subunit composition of mammalian transient receptor potential channels in living cells. *Proc Natl Acad Sci U S A*. 2002;99:7461–7466.
22. Lucas P, Ukhanov K, Leinders-Zufall T, Zufall F. A diacylglycerol-gated cation channel in vomeronasal neuron dendrites is impaired in *TRPC2* mutant mice: mechanism of pheromone transduction. *Neuron*. 2003;40:551–561.
23. Onohara N, Nishida M, Inoue R, Kobayashi H, Sumimoto H, Sato Y, Mori Y, Nagao T, Kurose H. TRPC3 and TRPC6 are essential for angiotensin II-induced cardiac hypertrophy. *EMBO J*. 2006;25:5305–5316.
24. Poburko D, Liao C-H, Lemos VS, Lin E, Maruyama Y, Cole WC, van Breemen C. Transient receptor potential channel 6-mediated, localized cytosolic $[Na^+]$ transients drive Na^+/Ca^{2+} exchanger-mediated Ca^{2+} Entry in purinergically stimulated aorta smooth muscle cells. *Circ Res*. 2007;101:1030–1038.
25. Iwamoto T, Kita S, Zhang J, Blaustein MP, Arai Y, Yoshida S, Wakimoto K, Komuro I, Katsuragi T. Salt-sensitive hypertension is triggered by Ca^{2+} entry via Na^+/Ca^{2+} exchanger type-1 in vascular smooth muscle. *Nat Med*. 2004;10:1193–1199.
26. Thebault S, Flourakis M, Vanoverberghe K, Vandermoere F, Roudbaraki M, Lehen'kyi V, Slomianny C, Beck B, Mariot P, Bonnal JL, Mauroy B, Shuba Y, Capiod T, Skryma R, Prevarskaya N. Differential role of transient receptor potential channels in Ca^{2+} entry and proliferation of prostate cancer epithelial cells. *Cancer Res*. 2006;66:2038–2047.
27. Trebak M, Hempel N, Wedel BJ, Smyth JT, Bird GS, Putney JW, Jr. Negative regulation of TRPC3 channels by protein kinase C-mediated phosphorylation of serine 712. *Mol Pharmacol*. 2005;67:558–563.
28. Kwan HY, Huang Y, Yao X. Protein kinase C can inhibit TRPC3 channels indirectly via stimulating protein kinase G. *J Cell Physiol*. 2006;207:315–321.
29. Kwan HY, Huang Y, Yao X. Regulation of canonical transient receptor potential isoform 3 (TRPC3) channel by protein kinase G. *Proc Natl Acad Sci U S A*. 2004;101:2625–2630.
30. Takahashi S, Lin H, Geshi N, Mori Y, Kawarabayashi Y, Takami N, Mori MX, Honda A, Inoue R. Nitric oxide-cGMP-protein kinase G pathway negatively regulates vascular transient receptor potential channel TRPC6. *J Physiol*. 2008;586:4209–4223.
31. Nishida M, Sugimoto K, Hara Y, Mori E, Morii T, Kurosaki T, Mori Y. Amplification of receptor signalling by Ca^{2+} entry-mediated translocation and activation of PLCγ2 in B lymphocytes. *EMBO J*. 2003;22:4677–4688.
32. Nishida M, Sato Y, Uemura A, Narita Y, Tozaki-Saitoh H, Nakaya M, Ide T, Suzuki K, Inoue K, Nagao T, and Kurose H. $P2Y_6$ Receptor-$G\alpha_{12/13}$ signaling in cardiomyocytes triggers pressure overload-induced cardiac fibrosis. *EMBO J*. 2008;27:3104–3115.
33. Bi D, Nishimura J, Niiro N, Hirano K, Kanaide H. Contractile properties of the cultured vascular smooth muscle cells: the crucial role played by RhoA in the regulation of contractility. *Circ Res*. 2005;96:890–897.
34. Large RA. Receptor-operated Ca^{2+} permeable nonselective cation channels in vascular smooth muscle: a physiologic perspective. *J Cardiovasc Electrophysiol*. 2002;13:493–501.
35. Inoue R, Jensen LJ, Shi J, Morita H, Nishida M, Honda A, Ito Y. Transient receptor potential channels in cardiovascular function and disease. *Circ Res*. 2006;99:119–131.
36. Schwede F, Maronde E, Genieser H, Jastorff B. Cyclicnucleotide analogs as biochemical tools and prospective drugs. *Pharmacol Ther*. 2000;87:199–226.
37. Nishida M, Watanabe K, Sato Y, Nakaya M, Kitajima K, Ide T, Inoue R, and Kurose H. Phosphorylation of TRPC6 channels at Thr^{69} is required for anti-hypertrophic effects of phosphodiesterase 5 inhibition. *J Biol Chem*. 2010;285:13244–13253.
38. Ambudkar IS. Ca^{2+} signaling microdomains: platforms for the assembly and regulation of TRPC channels. *Trends Pharmacol Sci*. 2006;27:25–32.
39. Hirano K, Hirano M, Kanaide H. Regulation of myosin phosphorylation and myofilament Ca^{2+} sensitivity in vascular smooth muscle. *J Smooth Muscle Res*. 2004;40:219–236.
40. Singh I, Knezevic N, Ahmmed GU, Kini V, Malik AB, Mehta D. $G\alpha_q$-TRPC6-mediated Ca^{2+} entry induces RhoA activation and resultant endothelial cell shape change in response to thrombin. *J Biol Chem*. 2007;282:7833–7843.
41. Nakamura K, Ikomi F, Ohhashi T. Cilostazol, an inhibitor of type 3 phosphodiesterase, produces endothelium-independent vasodilation in pressurized rabbit cerebral penetrating arterioles. *J Vasc Res*. 2006;43:86–94.

Supplementary Materials and Methods

Animals, Materials and Antibodies

All experiments on male Sprague-Dawley rats (240-330 g) were performed in accordance with the Guide for the Care and Use of Laboratory Animals prepared by Kyushu University. Poly-L-lysine, cilostazol, 1-oleoyl-2-acetyl-*sn*-glycerol (OAG), adenosine triphosphate (ATP), phenylephrine (α1 adrenergic receptor agonist), 9,11-dideoxy-11α,9α-epoxymethano-prostaglandin $F_{2\alpha}$ (U46619; thromboxane A2 analogue), cilostazol, milrinone, ionomycin, SK&F96365, 8-Bromo-cAMP, forskolin, KT5823, KT5720, and ascorbic acid were purchased from Sigma. Go6976 and KB-R7943 were from Carbiochem. Fugene 6 was from Roche. Pentobarbital was from Dainippon-Sumitomo Pharm. Fura2-AM was from Dojindo. Ang II was from Peptide Inst. CV11974 was provided from Takeda Chemical Industry. EGTA was from Nacalai. Cellmatrix type I-P was from Nitta Gelatin. Neutralized formaldehyde was from Wako. The cDNAs coding mouse TRPC6 and TRPC6-T69A mutant were constructed as described (1, 2). Anti-GFP antibody was from Abcam, anti-TRPC6 antibody was from Alomone, and protein A sepharose beads were from GE Healthcare. Phospho-Thr^{69} TRPC6 antiserum and phospho-Ser TRPC3/6/7 antiserum were generated against phospho-TRPC6 peptide (CHRRQ(p)TILREK) (3) and phospho-TRPC3/6/7 peptide (CKNDYRKL(p)SMQ). These phospho-specific antibodies were purified by antigen column. Anti-PDE3 antibody was from FabGennix Inc., and anti-PKA catalytic subunit (Cα) antibody was from BD Transduction Laboratory. Anti-RhoA, anti-mouse IgG and anti-rabbit IgG antibodies were from Santa Cruz.

Isometric Force Measurements of Rat Aortic Rings and Reconstituted Rings

Rats were anaesthetized with sodium pentobarbital (50 mg/kg, i.p.) and descending thoracic aorta was carefully isolated, cleaned of any adhering connective tissue, and cut into 3-mm-long rings. Each ring was mounted between a pair of triangular stainless steel hooks, one of which was stationary and the other was connected to a strain-gauge transducer (UL10GR, Minebea), and the isometric tension was recorded (MC6625, Graphtec, Tokyo, Japan). The rings, placed in 20 ml organ baths containing Krebs Henseleit (KH) solution maintained at 37 °C and aerated continuously with 95% O_2 and 5% CO_2, were stretched to a resting tension of 1.5 g and allowed to equilibrate for at least 30 min with occasional changes of KH solution. After equilibration, rings were set at 1.5 g and treated with or without cilostazol for 20 min. Then, the rings were re-set at 1.5 g and incubated for 10 min. We confirmed that the tension before agonist stimulation was 1.5 $\pm$ 0.1 g. The endothelium was removed from some preparations by gentle rubbing of the intimal surface with a paper swab moistened with KH solution. The presence or absence of endothelium was confirmed by examining the relaxations in response to acetylcholine (1 μM) of aortic rings precontracted by KCl (60 mM).

Production of a Reconstituted Ring and Measurement of Tension

Production of a reconstituted ring and measurement of tension were performed as described previously (4). The cultured primary rat aortic smooth muscle cells were collected with trypsinization and transfected with pCIneo vector encoding wild type TRPC6 or TRPC6 (T69A) mutant and pEGFP-N1 using electroporation (1400V, 10 msec x 3, Digital-Bio). Then cell suspensions were mixed with the culture medium (5 x

10^6 cells/ml) containing 0.6 mg/ml type I collagen (Cellmatrix Type I-P). For the expression of TRPC6 (3A) mutant (5), trypsinized cells were infected with adenoviruses encoding GFP or TRPC6 (3A) at 100 MOI in serum-free culture medium for 30 min and then mixed with collagen-containing culture medium. The mixture (100 μl, 0.5 x 10^6 cells) was placed around a silicone column (ϕ = 2 mm), which was attached on the center of the silicone disc (ϕ = 8 mm). After the collagen gel became solid, the culture medium was added and cultured for 24-48 h. The ring preparation so obtained was used for measurements of isometric tension development. We counted GFP-positive RAoSMCs using fluorescent microscopy and determined the transfection efficiency of electroporation was 70 ± 5% and that of adenoviral infection was more than 90% in monolayer-cultured RAoSMCs plated on the colaggen-coated glass-base dish.

For the tension recordings, the reconstituted rings were mounted onto two tungsten wires by passing the wires through the lumen of the rings. The resting tension was adjusted to 22 mg in Tyrode solution (NaCl 118 mM, KCl 5.4 mM, D-Glucose 10 mM, Hepes 10 mM, NaH_2PO_4 0.373 mM, $MgCl_2$ 2 mM, $CaCl_2$ 2 mM, taurine 1.5 mM). The rings were allowed to equilibrate for 60 min before starting experiments. Changes in tension were recorded isometrically through force displacement transducer (UL-2GR, Minebea).

Immunoprecipitation and Western Blot Analysis

HEK293 cells plated on 10 cm plates were harvested with 1 ml of RIPA buffer. Cell lysates were homogenized and supernatants were fractionated by centrifugation for

3 min at 10,000 rpm. GFP-fused proteins were immunoprecipitated in supernatants containing anti-GFP antibody (1.5 μl) in the presence of a 20 μl bed volume of protein A Sepharose beads rocking for 2 h at 4 °C (6). The immune complex were washed three times with RIPA buffer and resuspended with 80 μl of SDS sample buffer. For Western blotting, TRPC6-expressing HEK293 cells (3 x 10^5 cells) plated on 6 well dishes were directly harvested with 2 x SDS sample buffer (200 μl). After centrifugation, supernatants (20-40 μl) were fractionated by 8% SDS-PAGE gel and then transferred onto PVDF membrane. The expression and phosphorylation of endogenous TRPC6 proteins were detected by anti-TRPC6 (dilution rate: 1/1000) and anti-phospho-TRPC6 (1/1000) antibodies (3). The reactive bands were visualized using Supersignal® West Pico Luminol/Enhancer solution (Pierce). The optical density of the film was scanned and measured with Scion Image Software.

Measurement of Rho Activity

Activation of small G proteins was determined as described previously (7, 8). Activated Rho was pulled down with 10 μg of GST-fused Rho-binding domain of Rhotekin and 20 μl bed volume of glutathione Sepharose beads. Pull-downed Rho was detected with anti-RhoA antibody.

Reference

1. Inoue R, Okada T, Onoue H, Hara Y, Shimizu S, Naitoh S, Ito Y, Mori Y. The transient receptor potential protein homologue TRP6 is the essential component of vascular α1-adrenoceptor-activated Ca^{2+}-permeable cation channel. *Circ Res*. 2001; 88:325-32.
2. Takahashi S, Lin H, Geshi N, Mori Y, Kawarabayashi Y, Takami N, Mori MX, Honda A, Inoue R. Nitric oxide-cGMP-protein kinase G pathway negatively regulates vascular transient receptor potential channel TRPC6. *J Physiol.* 2008; 586:4209-23.
3. Nishida M, Watanabe K, Sato Y, Nakaya M, Kitajima N, Ide T, Inoue R, Kurose H. Phosphorylation of TRPC6 channels at Thr^{69} is required for anti-hypertrophic effects of phosphodiesterase 5 inhibition. *J Biol Chem.* 2010; 285:13244-13253.
4. Bi D, Nishimura J, Niiro N, Hirano K, Kanaide H. Contractile properties of the cultured vascular smooth muscle cells: the crucial role played by RhoA in the regulation of contractility. *Circ Res*. 2005; 96:890-897.
5. Onohara N, Nishida M, Inoue R, Kobayashi H, Sumimoto H, Sato Y, Mori Y, Nagao T, Kurose H. TRPC3 and TRPC6 are essential for angiotensin II-induced cardiac hypertrophy. *EMBO J*. 2006; 25:5305-16.
6. Nishida M, Sugimoto K, Hara Y, Mori E, Morii T, Kurosaki T, Mori Y. Amplification of receptor signalling by Ca^{2+} entry-mediated translocation and activation of PLCγ2 in B lymphocytes. *EMBO J*. 2003;22:4677-4688.
7. Nishida M, Tanabe S, Maruyama Y, Mangmool S, Urayama K, Nagamatsu Y, Takagahara S, Turner JH, Kozasa T, Kobayashi H, Sato Y, Kawanishi T, Inoue R, Nagao T & Kurose H. $G\alpha_{12/13}$-and reactive oxygen species-dependent activation of

c-Jun NH_2-terminal kinase and p38 MAPK by angiotensin receptor stimulation in rat neonatal cardiomyocytes. *J Biol Chem.* 2005;280:18434-18441.

8. Nishida M, Sato Y, Uemura A, Narita Y, Tozaki-Saitoh H, Nakaya M, Ide T, Suzuki K, Inoue K, Nagao T & Kurose H. $P2Y_6$ Receptor-$G\alpha_{12/13}$ Signaling in Cardiomyocytes Triggers Pressure Overload-induced Cardiac Fibrosis. *EMBO J.* 2008;27:3104-3115.

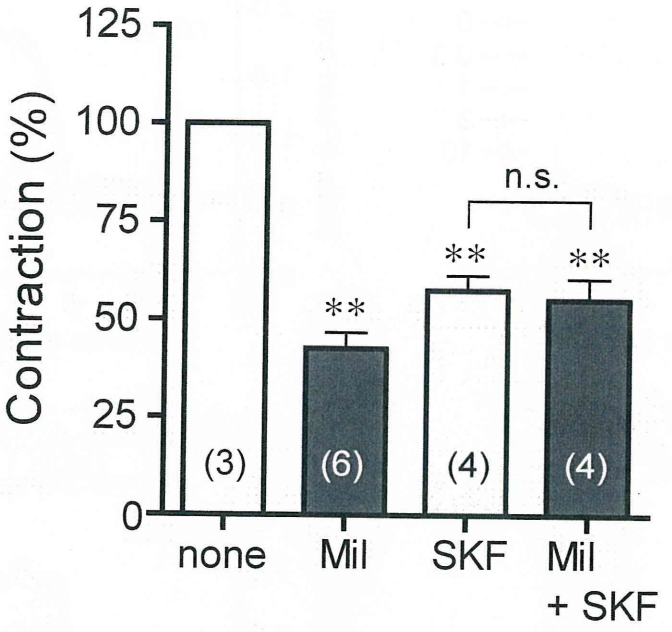

Supplemental Figure I. Milrinone suppresses Ang II-induced vasoconstriction by inhibiting of Ang II-induced Ca^{2+} influx. Ang II-induced contraction in the aortas pretreated with SK&F96365 (SK&F; 7 μM) with or without milrinone (Mil; 5 μM) for 30 min before Ang II stimulation. **; $P < 0.01$ vs control (none), n.s.; not significant.

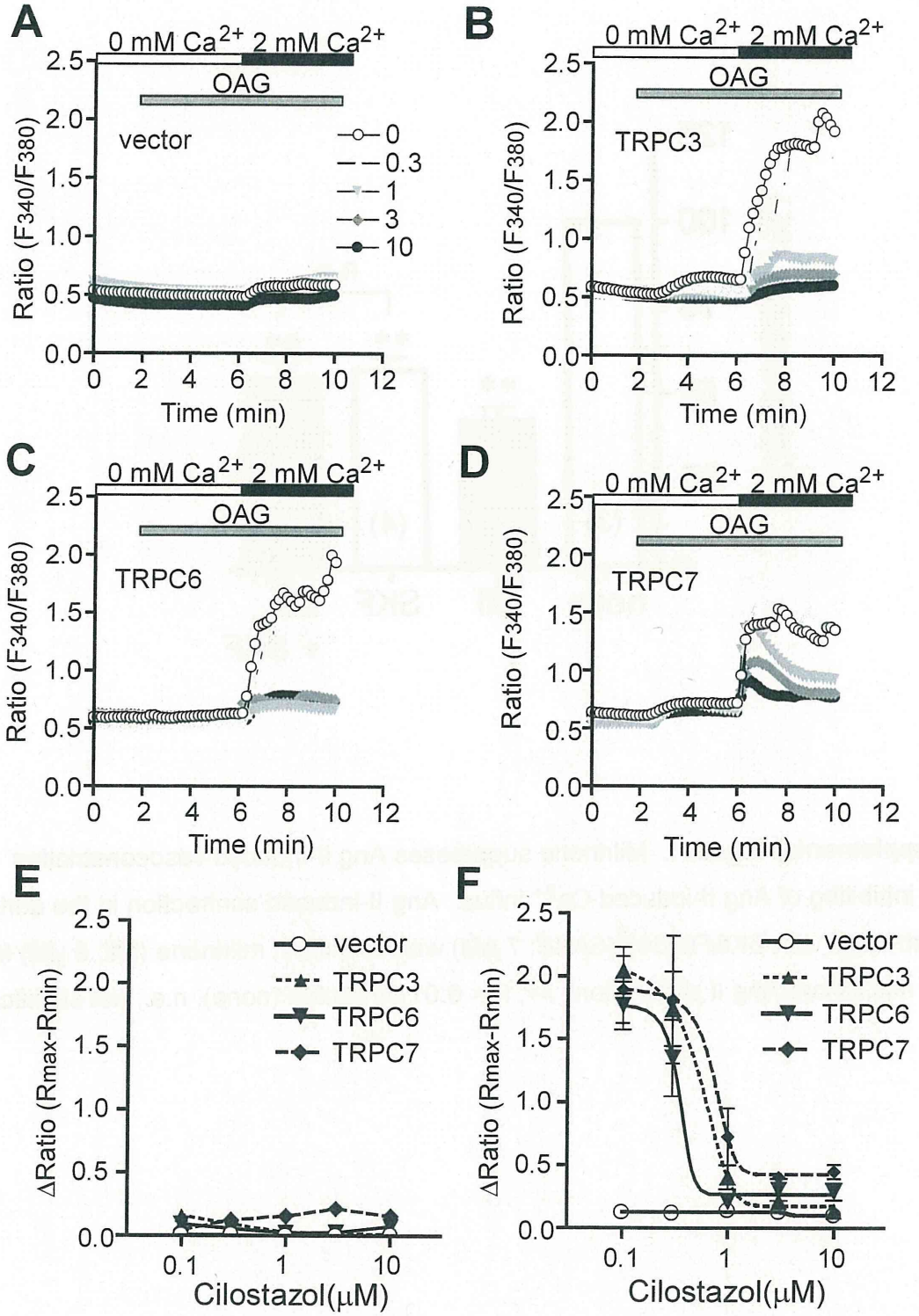

Supplemental Figure II. Suppression of DAG-mediated Ca^{2+} influx by PDE3 inhibition. (A-D) Average time courses of Ca^{2+} responses induced by DAG (1-oleoyl-2-acetyl-sn -glycerol, OAG) (30 μM) in the absence or presence of extracellular Ca^{2+} in vector (A), TRPC3 (B), TRPC6 (C), and TRPC7 (D)-overexpressing HEK293 cells. Cells were pretreated with indicated concentration of cilostazol (CLZ) for 30 min before OAG treatment. (E, F) Peak Ca^{2+} release-mediated increases in $[Ca^{2+}]_i$ (E) and Ca^{2+} influx -mediated increases in $[Ca^{2+}]_i$ (F) induced by OAG in the presence or absence of CLZ. N=42-76 cells.

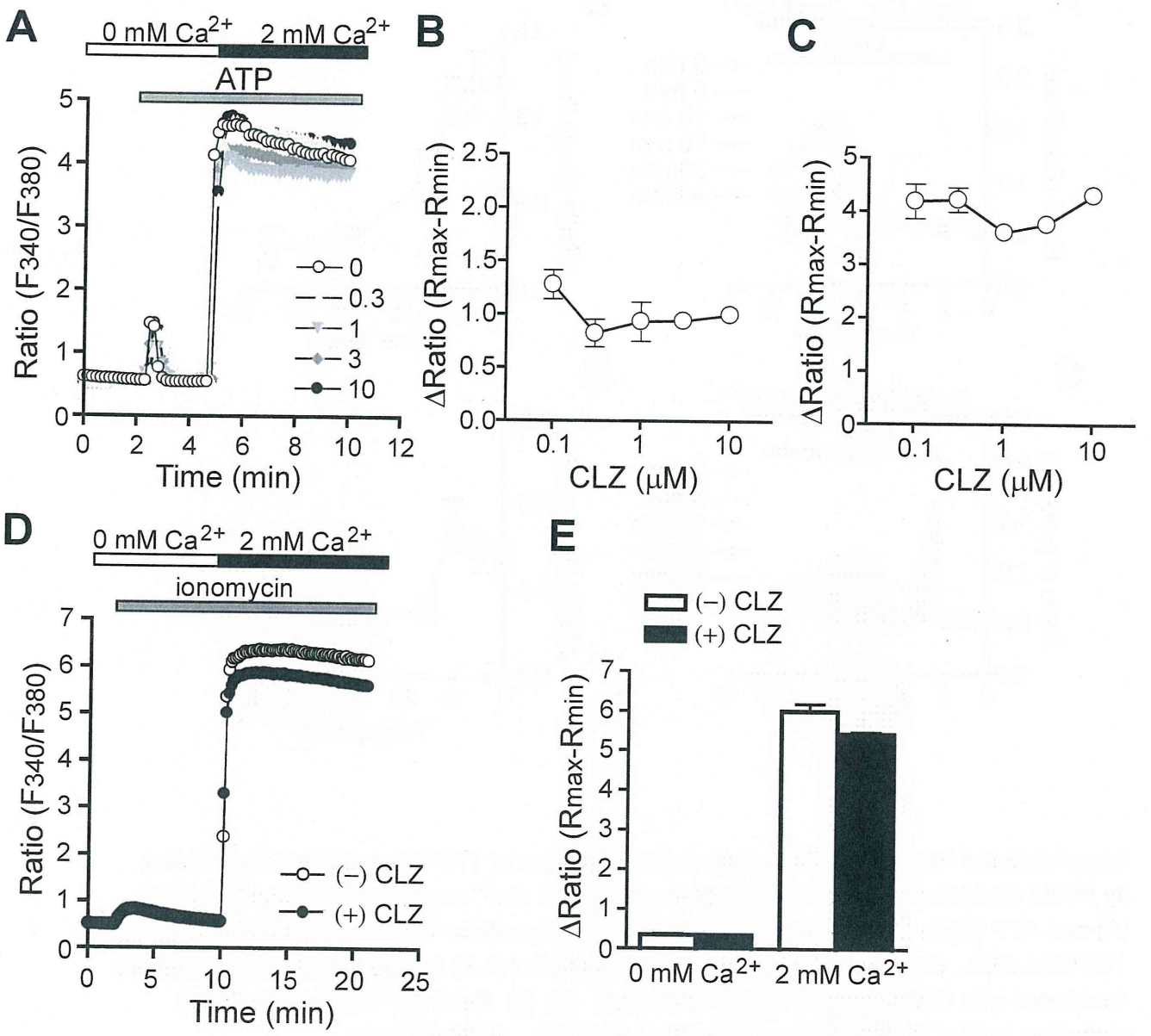

Supplemental Figure III. Inhibition of PDE3 does not suppress DAG-independent Ca^{2+} influx. (A-C) Effects of cilostazol (CLZ) on TRPC5-mediated Ca^{2+} influx induced by ATP stimulation. (A) Average time courses of Ca^{2+} responses induced by ATP in TRPC5-GFP-overexpressing HEK293 cells. (B, C) Peak changes in $[Ca^{2+}]_i$ induced by ATP in the absence (B) or presence (C) of extracellular Ca^{2+} (2 mM). (D, E) Effects of cilostazol on Ca^{2+} influx induced by store depletion. Cells were pretreated with CLZ (10 μM) for 30 min before ionomycin treatment. (D) Average time courses of Ca^{2+} responses induced by ionomycin (1 μM) in the absence or presence of extracellular Ca^{2+}. (E) Peak increases in $[Ca^{2+}]_i$ induced by ionomycin. N=108-136 cells.

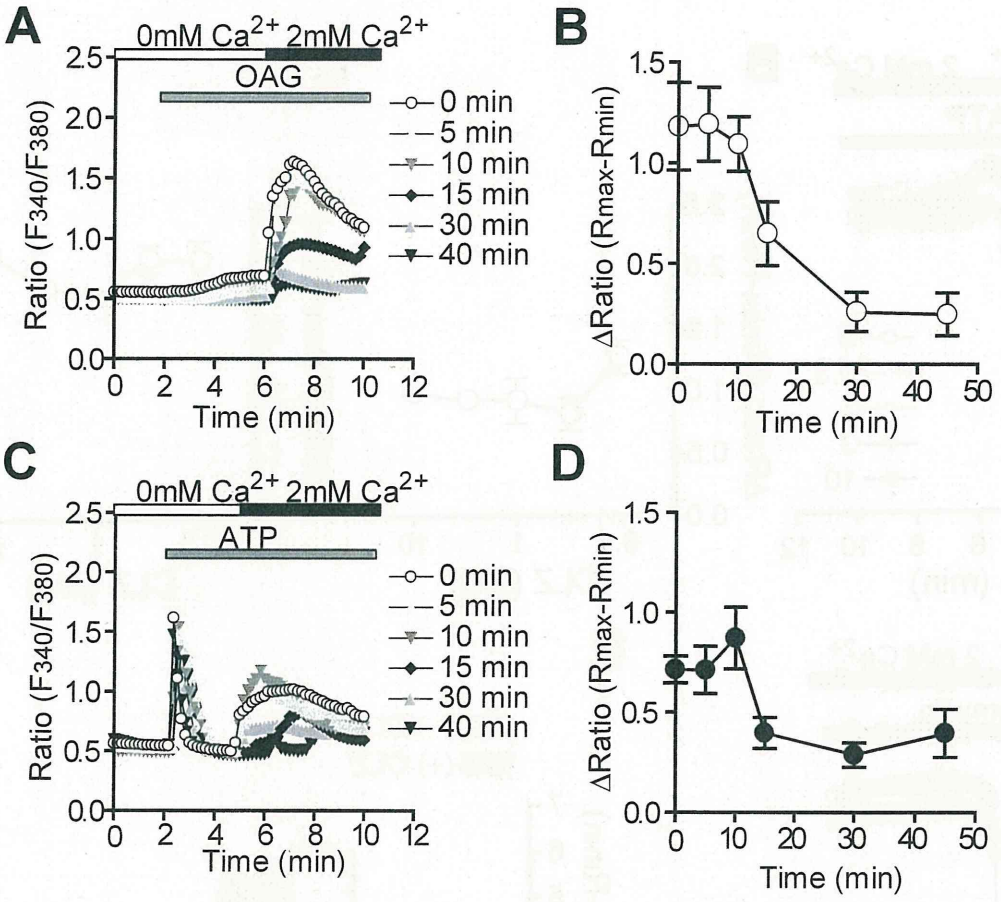

Supplemental Figure IV. Time-dependent inhibition of TRPC6-mediated Ca^{2+} influx by PDE3 inhibition. (A, C) Average time courses of Ca^{2+} responses induced by OAG (A) and ATP (C) in the absence or presence of extracellular Ca^{2+} in TRPC6-expressing HEK293 cells. Cells were pretreated with cilostazol (CLZ) for the indicated time before treatment with OAG (30 μM) or ATP (100 μM). (B, D) Peak Ca^{2+} influx-mediated increases in $[Ca^{2+}]_i$ induced by OAG (B) or ATP (D). N=69-92 cells.

Supplemantal Figure IV Nishioka et al.

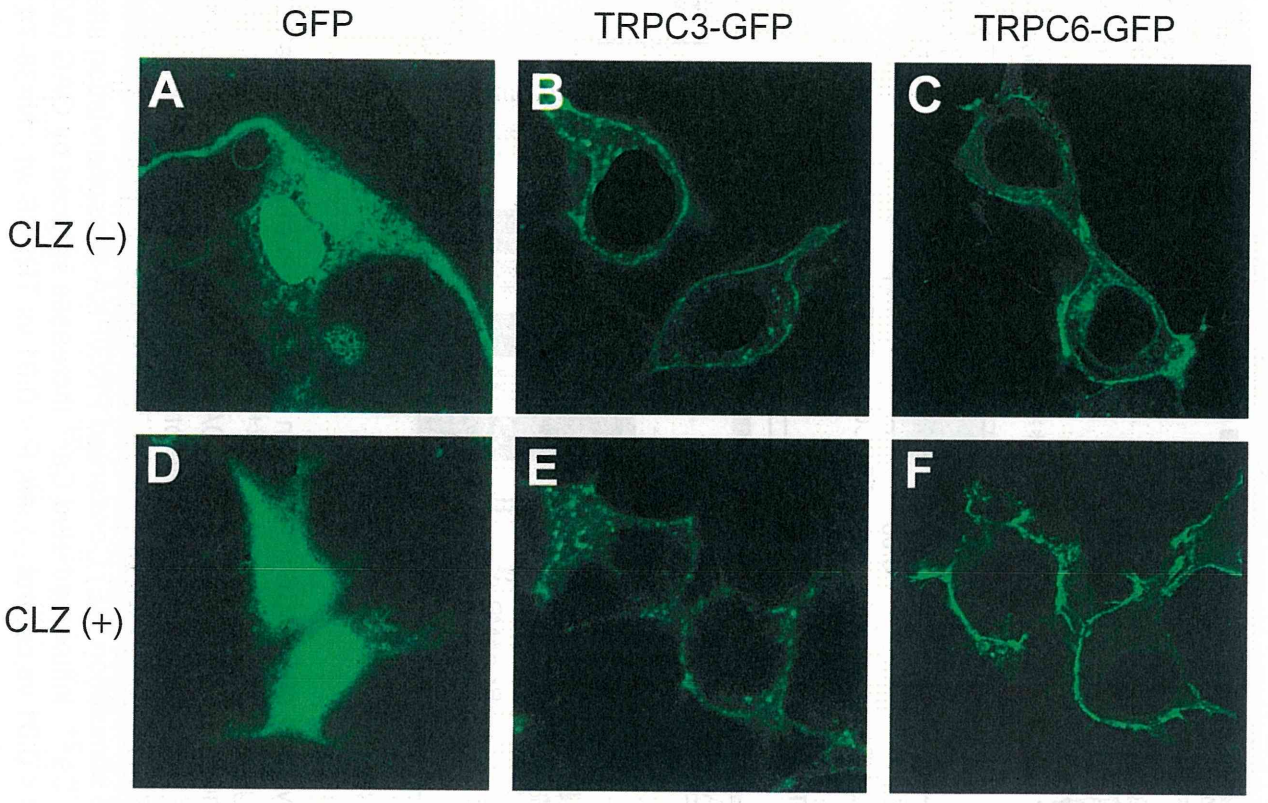

Supplemental Figure V. Inhibition of PDE3 does not affect membrane localization of TRPC3 and TRPC6 proteins. (A-F) Visualization of GFP (A, D), GFP-fused TRPC3 (B, E) and GFP-fused TRPC6 (C, F) proteins in the absence (A-C) or presence (D-F) of cilostazol (CLZ). Cells were treated with CLZ (1 μM) for 30 min. N=3 experiments.

Supplemental Figure V Nishioka et al.

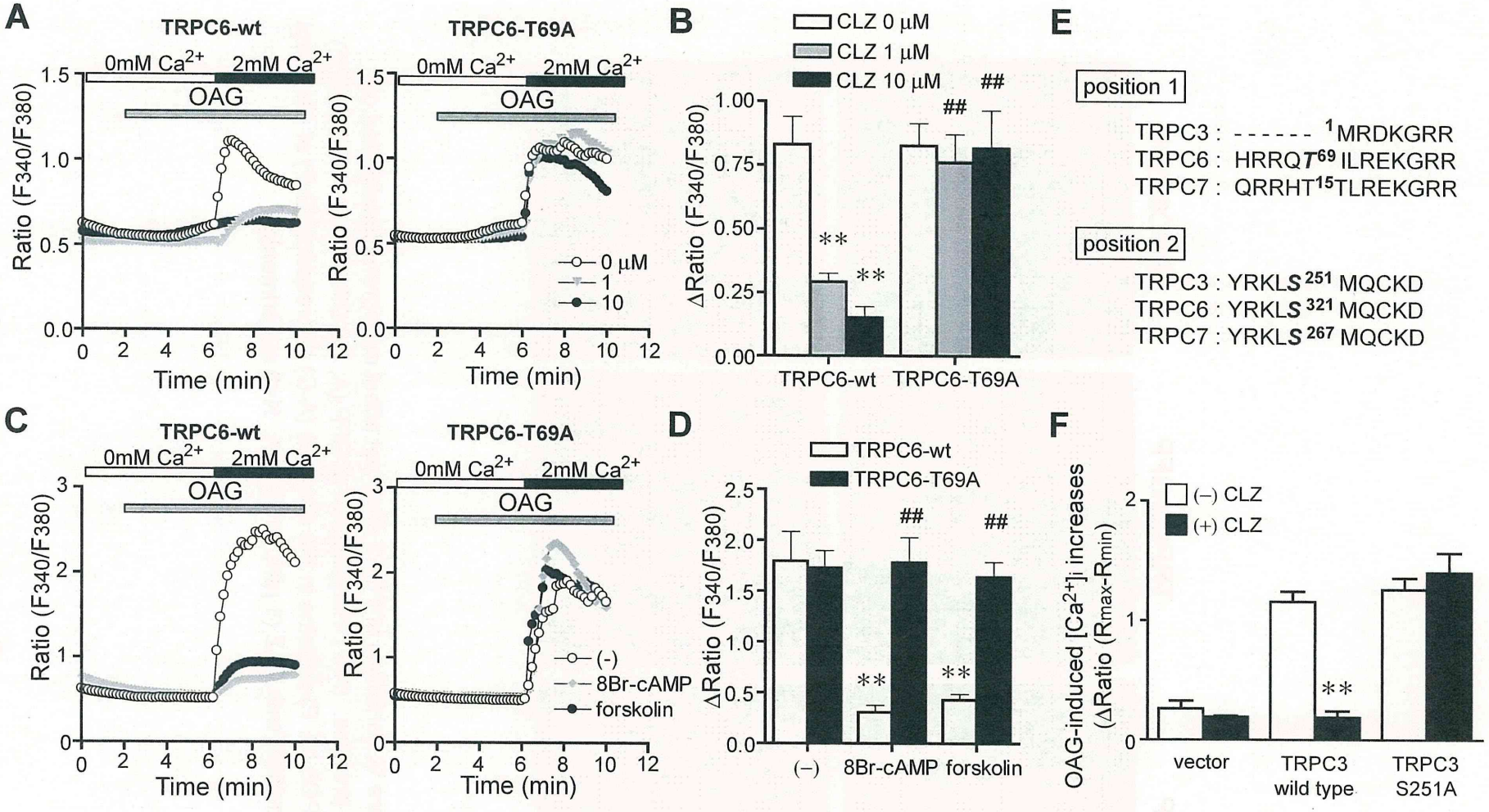

Supplemental Figure VI. Involvement of phosphorylation of TRPC6 at Thr69 in suppression of DAG-mediated Ca^{2+} influx by PDE3 inhibition. (A, B) Effects of CLZ on DAG (1-oleoyl-2-acetyl-sn-glycerol, OAG)-induced Ca^{2+} influx in wild type TRPC6 (TRPC6-wt)- or TRPC6-T69A -expressing cells. (A) Average time courses of changes in $[Ca^{2+}]_i$ induced by OAG (30 μM). Cells were pretreated with CLZ for 30 min before OAG stimulation. (B) Peak increases in $[Ca^{2+}]_i$ induced by OAG in the presence of extracellular Ca^{2+}. (C, D) Average time courses (C) and Peak changes (D) of $[Ca^{2+}]_i$ induced by OAG in TRPC6-wt- or TRPC6-T69A-expressing cells. Cells were pretreated with 8-Br-cAMP (30 μM) or forskolin (10 μM) for 30 min before OAG stimulation. (E) Conserved PKG/PKA-phosphorylation sites in mouse TRPC3 (836 a.a.), TRPC6 (930 a.a.), and TRPC7 (862 a.a.). (F) Peak Ca^{2+} influx-mediated Ca^{2+} increases induced by OAG (30 μM) in vector-, wild type TRPC3-, and TRPC3-S251A-expressing HEK293 cells. **; $P < 0.01$ vs control (-), ##; $P < 0.01$ vs TRPC6-wt. N=38-74 cells.